

Appendix

SHG from vicinal Si(001) surfaces

Here we present the results of rotational-anisotropy SHG (RA-SHG) from vicinal Si(001) surfaces. The surface normal direction of the vicinal Si(001) sample is away from the principal [001] crystal axis for a small offset angle, α , which is named as vicinal angle, as shown in Fig. 2.2 in Chapter 2. Moreover, the offset direction is chosen to be in a mirror plane of symmetry of the Si crystal. The vicinal angle dependence of the (p, p) polarized RA-SHG signal is shown in Fig. A.1. The photon energy dependence of the RA-SHG signal from vicinal Si(001) surfaces for different polarization configurations are shown in Figs. A.2, A.3, A4, and A.5. These results will not only help improve the understanding of surface SHG, but will also help with the understanding of the step structures and energies on vicinal Si surfaces or interfaces.

The experimental conditions were the same as in Chapter 3, except that the spectroscopic studies here were also performed at higher photon energies, which were obtained by frequency doubling of the output of an OPO, as described in Chapter 1. All measurements were carried out at room temperature in a N_2 ambient.

Three sets of vicinal Si(001) samples were investigated. The first set were natively oxidized vicinal Si(001) samples with different vicinal angles of 0° , 1° , 2° , 3° , 4° , and 5° , designated as NO-Si V. The [001] crystal direction of the vicinal (off axis) Si(001) wafer was off from the surface normal toward the [110] direction for a small vicinal angle. Two more sets of samples, the thermally oxidized vicinal Si(001) samples, designated as TO-Si V, and the hydrogen terminated vicinal Si(001) samples,

designated as H-Si V, were prepared from the NO-Si V samples with the same preparation conditions as in Chapter 3.

The theoretical predictions of the symmetry properties of the RA-SHG signals from vicinal Si(001) surfaces are shown as Eqs. (2.40a) and (2.40b) in Chapter 2. The SH intensity in all of the figures is normalized in the same way as that in Chapter 3. It is important to note that the azimuthal angle is defined to be between the plane of incidence and the projection of the [110] axis in the surface plane. Moreover, when the azimuthal angle $\psi = 0$, the incident beam is toward the downward miscut direction of the vicinal surface (or downward steps on the vicinal surface), as shown in Fig. 2.2 in Chapter 2.

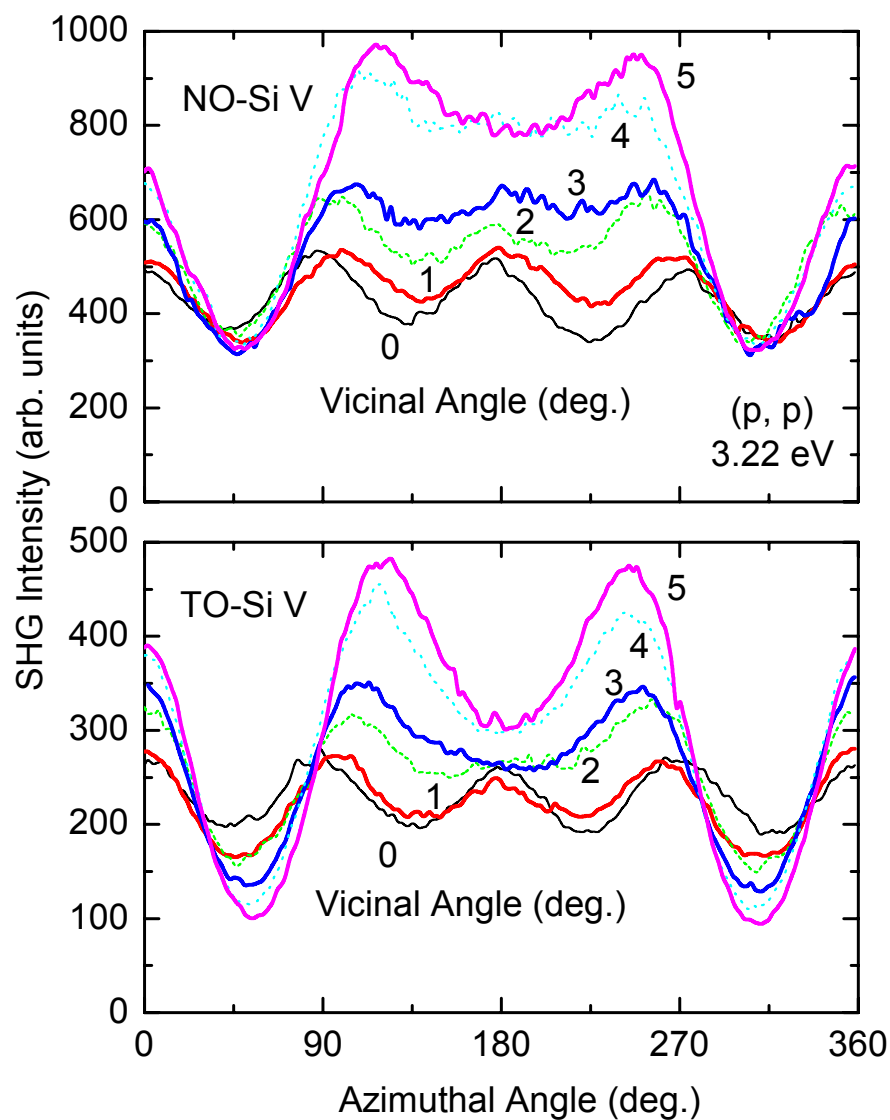


Fig. A.1. (p, p) polarized RA-SHG signals at a two-photon energy of 3.22 eV from natively oxidized vicinal Si(001) surfaces (NO-Si V) (upper panel) and thermally oxidized vicinal Si(001) surfaces (TO-Si V) (lower panel) with different vicinal angles of 0° , 1° , 2° , 3° , 4° , and 5° .

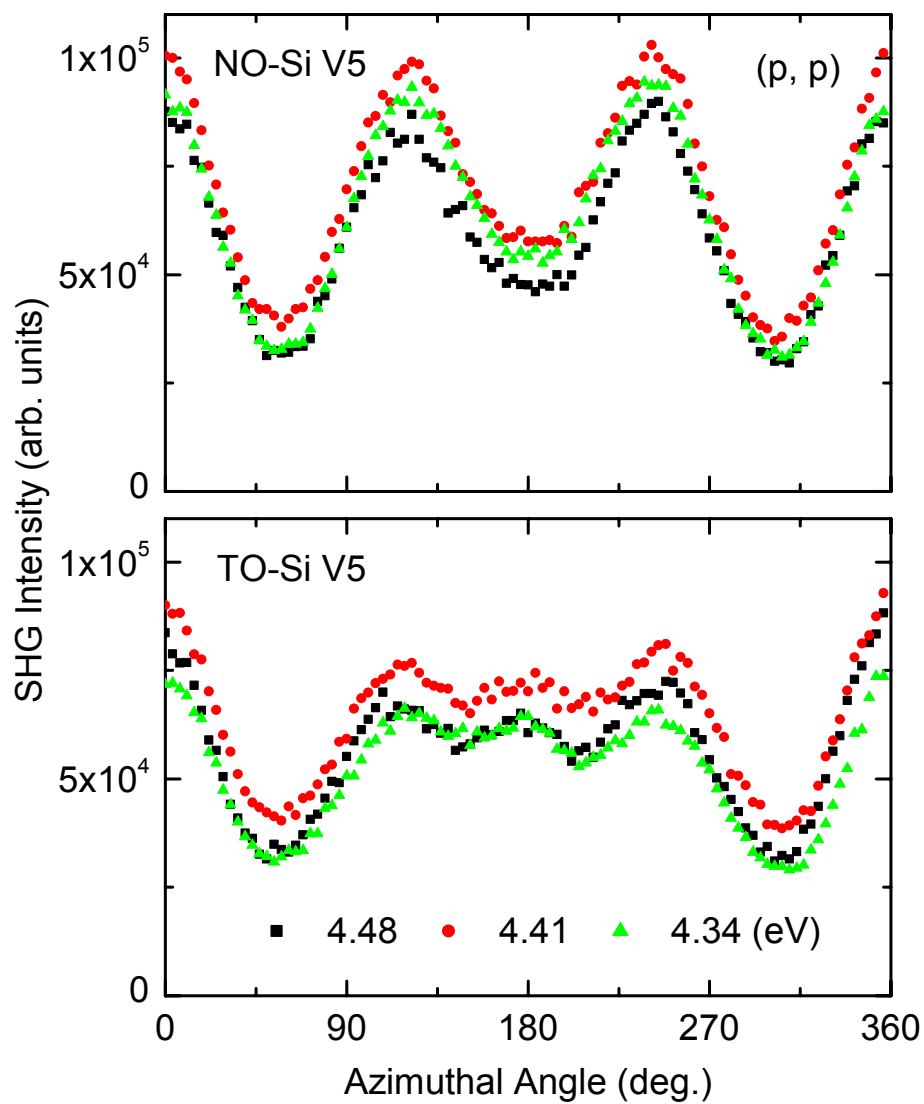


Fig. A.2. (p, p) polarized RA-SHG signals from a natively oxidized Si sample with vicinal angle of 5° (NO-Si V5) (upper panel) and a thermally oxidized Si sample with vicinal angle of 5° (TO-Si V5) (lower panel) at two-photon energies 4.34 eV, 4.41 eV, and 4.48 eV.

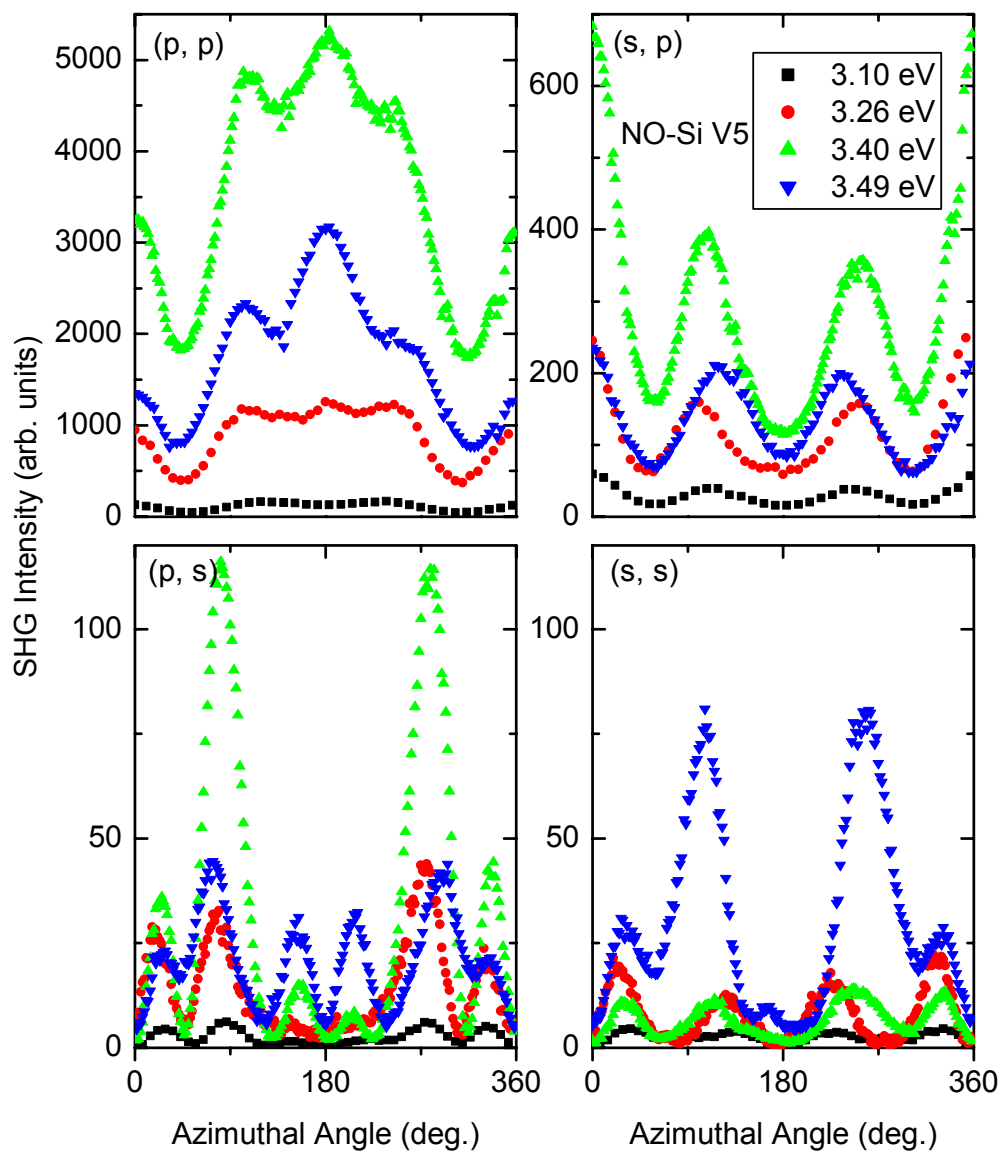


Fig. A.3. RA-SHG signals from a natively oxidized Si sample with vicinal angle of 5° (NO-Si V5) at several two-photon energies of 3.10 eV, 3.26 eV, 3.40 eV, and 3.49 eV for different polarizations: (p, p) , (s, p) , (p, s) , and (s, s) .

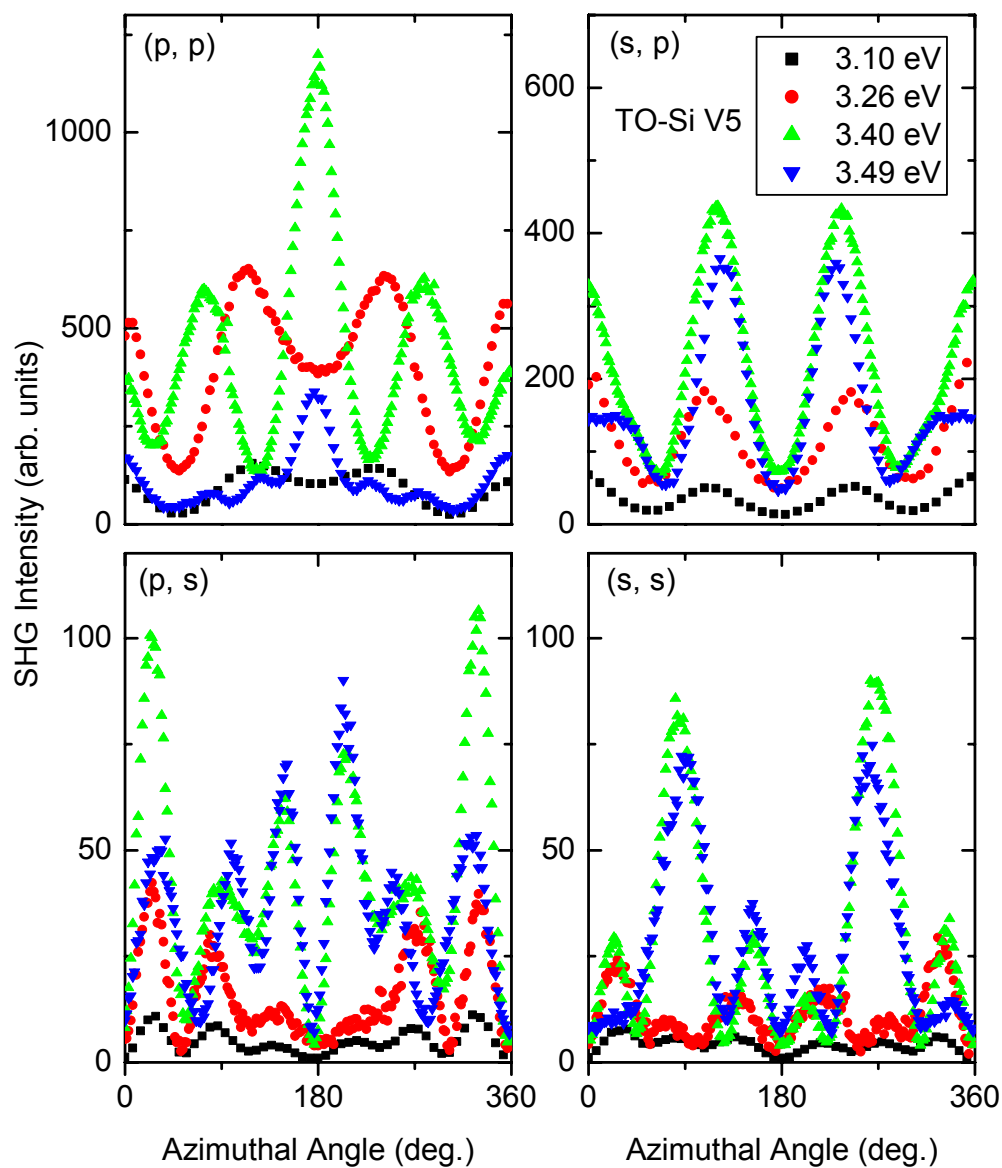


Fig. A.4. RA-SHG signal from a thermally oxidized Si sample with vicinal angle of 5° (TO-Si V5) at several two-photon energies of 3.10 eV, 3.26 eV, 3.40 eV, and 3.49 eV for different polarizations: (p, p) , (s, p) , (p, s) , and (s, s) .

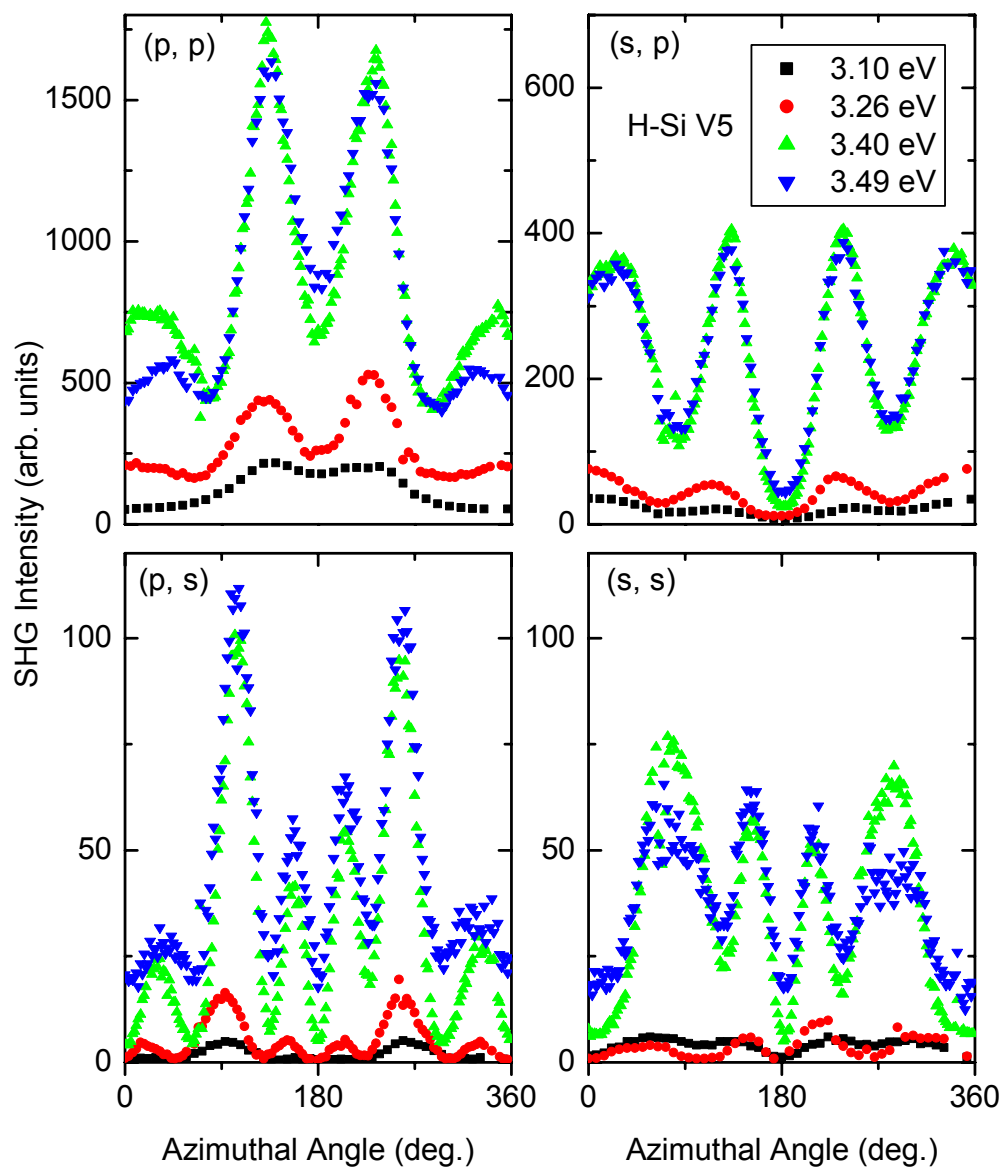


Fig. A.5. RA-SHG signal from a hydrogen terminated Si sample with vicinal angle of 5° (H-Si V5) at several two-photon energies of 3.10 eV, 3.26 eV, 3.40 eV, and 3.49 eV for different polarizations: (p, p) , (s, p) , (p, s) , and (s, s) .